

Electronic Supplementary Information

Sustainable at Both Ends: Electrochemical CO₂ Utilization Paired with Electrochemical Treatment of Nitrogenous Waste

Xenia V. Medvedeva,[‡] Jury J. Medvedev,[‡] Stephen W. Tatarchuk, Rachelle M. Choueiri and Anna Klinkova*

Department of Chemistry and Waterloo Institute for Nanotechnology, University of Waterloo, Waterloo, ON N2L 3G1, Canada

[‡] These authors contributed equally.

*Corresponding author: aklinkova@uwaterloo.ca

19 Pages, 3 Figures, and 15 Tables are included

Experimental Details

All reactions in this work were performed either in a two-compartment H-cell or a flow cell. H-cell was equipped with an anion exchange membrane (Fumasep FAB-PK-130, FuelCellStore), Ag cathode prepared by chemical vapor deposition, and a Ni-foam anode (McMaster-Carr) or Pt/C anode (60% platinum on carbon, FuelCellStore). Flow cell was equipped with an anion exchange membrane (Fumasep FAB-PK-130, FuelCellStore), Ag coated gas diffusion layer (GDL) prepared by chemical vapor deposition, and a Ni-foam anode. Electrochemical cells were connected to an electrochemical workstation (Biologic SP-300). Potentials were reported relative to Ag-wire (Ag/Ag⁺; this quasi-reference electrode was also calibrated with Fc/Fc⁺ redox couple; for the details see [1]) for organic electrolytes, and relative to Ag/AgCl (3.5M KCl) electrode for aqueous electrolytes. To analyze product distribution, reactions were performed at constant current densities or potentials. Gas products were analyzed using Agilent 7890B GC System; liquid products were analyzed by NMR of crude reaction mixtures with an internal standard. Details of the analysis are reported elsewhere [1].

Calculation of Gibbs free energies and cell potentials of electrochemical reactions

To identify energy-saving alternatives to the OER, standard Gibbs free energies of selected coupled reactions ($\Delta G^{\circ}_{\text{reaction}}$) and their corresponding standard cell potentials (E°_{cell}) have been calculated (equations 1 and 2). Gibbs free energy of formation (ΔG°_f) values for products and reactants were taken from the literature data or estimated by the Joback method (Table S1). [2-6] This method allows to predict pure-component properties from group-contributions. [3] ΔG°_f values for glycolic acid, (bromomethyl)benzene and 2-phenylacetic acid were estimated by the Joback method using a designated online software [4].

$$E^{\circ}_{\text{cell}} = \frac{-\Delta G^{\circ}_{\text{reaction}}}{nF} \quad \#(1)$$

Where E°_{cell} – standard cell potential, $\Delta G^{\circ}_{\text{reaction}}$ – standard-state free energy of reaction, n – number of electrons transferred, F – Faraday constant;

$$\Delta G^{\circ}_{\text{reaction}} = \sum v_{\text{product}} \times \Delta G^{\circ}_{f,\text{product}} - \sum v_{\text{reactant}} \times \Delta G^{\circ}_{f,\text{reactant}} \quad \#(2)$$

Where v is the stoichiometric coefficient and ΔG°_f is the Gibbs free energy of formation.

For each anodic process, only one product of oxidation was considered: oxygen for water oxidation, acetic acid for ethanol oxidation, glycolic acid for ethylene glycol oxidation, formic acid for glycerol oxidation, gluconic acid for glucose oxidation, nitrogen and carbon dioxide for urea oxidation reaction (UOR), and nitrogen for ammonia oxidation reaction (AOR). Half-reactions for anodic and cathodic processes (Table S2, S3) were given for an alkaline media.

Table S1. Gibb's free energy of formation ($\Delta G^{\circ f}$) values.

Compound	Molecular formula	$\Delta G^{\circ f}$ (kJ mol ⁻¹)	Reference
Water	H ₂ O	-237.14	[2]
Carbon dioxide	CO ₂	-394.4	[2]
Carbon monoxide	CO	-137.16	[2]
Ethanol	C ₂ H ₅ OH	-174.8	[2]
Acetic acid	CH ₃ CO ₂ H	-390.2	[2]
Ethylene glycol	C ₂ H ₆ O ₂	-323.2	[2]
Glycolic acid	C ₂ H ₄ O ₃	-436.6	[3,4]*
Glycerol	C ₃ H ₈ O ₃	-477.0	[2]
Formic acid	HCOOH	-361.4	[2]
Glucose	C ₆ H ₁₂ O ₆	-910.4	[2]
Gluconic acid	C ₆ H ₁₂ O ₇	-1170	[5]
Urea	CO(NH ₂) ₂	-196.8	[2]
Ammonia (aq)	NH ₃	-26.57	[6]
Hydrobromic acid	HBr	-53.4	[2]
(Bromomethyl)benzene	C ₇ H ₇ Br	134.79	[3,4]*
2-Phenylacetic acid	C ₈ H ₈ O ₂	-136.85	[3,4]*

*Estimated by **Joback Method****Table S2.** Thermodynamic standard values of ΔG° _{reaction}, normalized ΔG° _{reaction}, and overall standard cell potential ($|E^{\circ}_{cell}|$) for the electroreduction of **CO₂ to CO** (**CO₂ + H₂O + 2e⁻ → CO + 2OH⁻**), coupled to anodic **oxygen evolution**, or **ethanol, ethylene glycol, glycerol, glucose, urea, and ammonia** electrooxidation.

Anodic reaction	Overall reaction, (electrons transferred)	ΔG° _{reaction} (kJ mol ⁻¹)	ΔG° _{reaction} normalized (kJ mol ⁻¹)*	$ E^{\circ}_{cell} $ (V)
2OH ⁻ →H ₂ O+1/2O ₂ +2e ⁻	CO ₂ →CO+1/2O ₂ (2e ⁻)	257.24	257.24	1.33
4OH ⁻ +C ₂ H ₅ OH→CH ₃ CO ₂ H+3H ₂ O+4e ⁻	2CO ₂ +C ₂ H ₅ OH→2CO+CH ₃ CO ₂ H+H ₂ O (4e ⁻)	61.94	30.97	0.16
4OH ⁻ + +(CH ₂ OH) ₂ →HOCH ₂ CO ₂ H+3H ₂ O+4e ⁻	2CO ₂ +(CH ₂ OH) ₂ →2CO+ HOCH ₂ CO ₂ H +H ₂ O (4e ⁻)	163.94	81.97	0.42
8OH ⁻ +C ₃ H ₈ O ₃ →3HCOOH+5H ₂ O+8e ⁻	4CO ₂ +C ₃ H ₈ O ₃ →4CO+3HCOOH +H ₂ O (8e ⁻)	184.62	46.16	0.24
2OH ⁻ +C ₆ H ₁₂ O ₆ →C ₆ H ₁₂ O ₇ +H ₂ O+2e ⁻	CO ₂ + C ₆ H ₁₂ O ₆ →CO+ C ₆ H ₁₂ O ₇ (2e ⁻)	6.24	6.24	0.03
6OH ⁻ +CO(NH ₂) ₂ →CO ₂ +N ₂ +5H ₂ O+6e ⁻	2CO ₂ + CO(NH ₂) ₂ →3CO+ N ₂ + 2H ₂ O (6e ⁻)	99.84	33.28	0.17
6OH ⁻ +2NH ₃ →N ₂ +6H ₂ O+6e ⁻	3CO ₂ + 2NH ₃ →3CO+ N ₂ + 3H ₂ O (6e ⁻)	113.44	37.81	0.2

*Gibbs free energy of the reaction divided by the number of CO₂ molecules in the overall reaction equation.

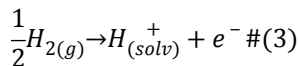
Table S3. Thermodynamic standard values of $\Delta G^{\circ}_{\text{reaction}}$ and $|E^{\circ}_{\text{cell}}|$ for the cathodic electrocarboxylation of **BnBr + CO₂ to RCO₂H** ($\text{BnBr} + \text{CO}_2 + 2\text{H}_2\text{O} + 2e^- \rightarrow \text{BnCO}_2\text{H} + \text{HBr} + 2\text{OH}^-$), coupled to the anodic **oxygen evolution**, or **ethanol, ethylene glycol, glycerol, glucose, urea, and ammonia** electrooxidation.

Anodic reaction	Overall reaction (electrons transferred)	$\Delta G^{\circ}_{\text{reaction}}$ (kJ mol ⁻¹)	$\Delta G^{\circ}_{\text{reaction}}$ normalized (kJ mol ⁻¹)*	$ E^{\circ}_{\text{cell}} $ (V)
$2\text{OH}^- \rightarrow \text{H}_2\text{O} + 1/2\text{O}_2 + 2e^-$	$\text{CO}_2 + \text{RBr} + \text{H}_2\text{O} \rightarrow \text{RCO}_2\text{H} + \text{HBr} + 1/2\text{O}_2 (2e^-)$	306.5	306.5	1.59
$4\text{OH}^- + \text{C}_2\text{H}_5\text{OH} \rightarrow \text{CH}_3\text{CO}_2\text{H} + 3\text{H}_2\text{O} + 4e^-$	$2\text{CO}_2 + 2\text{RBr} + \text{C}_2\text{H}_5\text{OH} + \text{H}_2\text{O} \rightarrow 2\text{RCO}_2\text{H} + 2\text{HBr} + \text{CH}_3\text{CO}_2\text{H} (4e^-)$	160.46	80.23	0.42
$4\text{OH}^- + (\text{CH}_2\text{OH})_2 \rightarrow \text{HOCH}_2\text{CO}_2\text{H} + 3\text{H}_2\text{O} + 4e^-$	$2\text{CO}_2 + 2\text{RBr} + (\text{CH}_2\text{OH})_2 + \text{H}_2\text{O} \rightarrow 2\text{RCO}_2\text{H} + 2\text{HBr} + \text{HOCH}_2\text{CO}_2\text{H} (4e^-)$	262.46	131.23	0.68
$8\text{OH}^- + \text{C}_3\text{H}_8\text{O}_3 \rightarrow 3\text{HCOOH} + 5\text{H}_2\text{O} + 8e^-$	$4\text{CO}_2 + 4\text{RBr} + \text{C}_3\text{H}_8\text{O}_3 + 3\text{H}_2\text{O} \rightarrow 4\text{RCO}_2\text{H} + 4\text{HBr} + 3\text{HCOOH} (8e^-)$	381.66	95.42	0.49
$2\text{OH}^- + \text{C}_6\text{H}_{12}\text{O}_6 \rightarrow \text{C}_6\text{H}_{12}\text{O}_7 + \text{H}_2\text{O} + 2e^-$	$\text{CO}_2 + \text{RBr} + \text{C}_6\text{H}_{12}\text{O}_6 + \text{H}_2\text{O} \rightarrow \text{RCO}_2\text{H} + \text{HBr} + \text{C}_6\text{H}_{12}\text{O}_7 (2e^-)$	55.5	55.5	0.29
$6\text{OH}^- + \text{CO}(\text{NH}_2)_2 \rightarrow \text{CO}_2 + \text{N}_2 + 5\text{H}_2\text{O} + 6e^-$	$2\text{CO}_2 + 3\text{RBr} + \text{CO}(\text{NH}_2)_2 + \text{H}_2\text{O} \rightarrow 3\text{RCO}_2\text{H} + 3\text{HBr} + \text{N}_2 (6e^-)$	247.62	82.54	0.43
$6\text{OH}^- + 2\text{NH}_3 \rightarrow \text{N}_2 + 6\text{H}_2\text{O} + 6e^-$	$3\text{CO}_2 + 3\text{RBr} + 2\text{NH}_3 \rightarrow 3\text{RCO}_2\text{H} + 3\text{HBr} + \text{N}_2 (6e^-)$	261.22	87.07	0.45

*Gibbs free energy of the reaction divided by the number of CO₂ molecules in the overall reaction equation.

Standard potentials in RHE and SHE scales [Ref. 7-10]

Standard potentials in aqueous media are relative to the hydrogen electrode – the oxidation of molecular hydrogen to solvated protons:



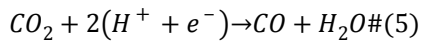
Two types of hydrogen electrodes are used in electrochemistry: the standard hydrogen electrode (SHE) and the reversible hydrogen electrode (RHE). The potential of SHE is zero under standard conditions (P = 1 bar, T = 298.15K, pH = 0). The RHE is defined to be in equilibrium at U = 0V at any pH, so additional pH correction is not needed.

The formation energy of proton-electron couple in RHE scale is defined by equation (4):

$$\Delta G^{\circ}_f(H^+ + e^-) = -F \times U_{\text{RHE}} \#(4)$$

where U_{RHE} is potential in RHE scale.

Electrochemical reduction of CO₂ to CO is described by the following equation:



The free energy of this reaction $\Delta G_{\text{CO2RR}}^{\circ}$ is:

$$\begin{aligned} & \Sigma v_{\text{products}} \times \Delta G^{\circ}_f(\text{products}) - \Sigma v_{\text{reagents}} \times \Delta G^{\circ}_f(\text{reagents}) - 2 \times \Delta G^{\circ}_f(H^+ + e^-) \\ &= \Delta G^{\circ}_f(\text{CO}) + \Delta G^{\circ}_f(\text{H}_2\text{O}) - \Delta G^{\circ}_f(\text{CO}_2) + 2F \times U_{\text{RHE}} \#(6) \end{aligned}$$

At the standard equilibrium potential $U_{CO_2RR}^{\circ}$ the free Gibbs energy is zero and equation (6) can be solved to give equation (7):

$$\begin{aligned} U_{CO_2RR}^{\circ} &= \frac{1}{2} (\Delta G_f^{\circ}(CO_2) - \Delta G_f^{\circ}(CO) - \Delta G_f^{\circ}(H_2O)) \\ &= \frac{1}{2} \times (-394.4 + 137.2 + 237.1) = -0.1V \text{ vs RHE} \#(7) \end{aligned}$$

The RHE equilibrium potential is constant at any pH, but electrochemical potential on the SHE scale involves only the energy of an electron (equation 8). Thus, if half-reaction involves protons, the pH correction is required.

$$U_{SHE} = -\frac{1}{F} \times \Delta G_f^{\circ}(e^-) \#(8)$$

where U_{SHE} is the potential in the SHE scale.

The difference between the RHE and SHE scales is defined by a simple equation (9):

$$U_{RHE} = U_{SHE} - \frac{1}{F} \times \Delta G_f^{\circ}(H^+) = U_{SHE} + 0.059 \times pH(V) \#(9)$$

The standard electrode potentials for half-reactions used in this work are summarized in Table S4. Most standard potentials of cathodic and anodic reactions were taken from literature. [11-16] Standard potentials for AOR and UOR on the RHE scale were calculated by analogy with equations (5)-(7) and converted to the SHE scale using the equation (9).

Table S4. Standard thermodynamic potentials of selected half-reactions in aqueous electrolytes.

Reaction	E° (vs RHE)	E° (vs SHE) pH = 7	E° (vs SHE) pH = 14
CO ₂ Reduction Reaction $CO_2 + 2H^+ + 2e^- \rightarrow CO + H_2O$	-0.1V	-0.51V	-0.93V
Oxygen Evolution Reaction $2H_2O \rightarrow O_2 + 4H^+ + 4e^-$	1.23V	-0.82V	-0.4V
Urea Oxidation Reaction $CO(NH_2)_2 + 6OH^- \rightarrow N_2 + 5H_2O + CO_2 + 6e^-$	0.07	-0.34V	-0.76V
Ammonia Oxidation Reaction $2NH_3 + 6OH^- \rightarrow N_2 + 6H_2O + 6e^-$	0.06	-0.35V	-0.77V

Performance of different electrocatalysts towards selected anodic and cathodic reactions (literature data)

Table S5. OER performance of selected electrocatalysts

Anode	E (V vs SHE)	E(V vs RHE)	Electrolyte	Ref
$\alpha\text{-Ni(OH)}_2/\text{CeO}_2$	0.64	1.47	1M KOH	[17]
Fe ²⁺ -NiFe LDH nanosheets	0.595	1.425	1M KOH	[18]
FeCoW oxyhydroxides	0.591	1.421	1M KOH	[19]
NiFe LDH nanoplatelets	0.624	1.454	1M KOH	[20]
Petaloid NiMn LDH nanosheets	0.62	1.45	1M KOH	[21]
Ultrathin CoMn LDH nanosheets	0.724	1.554	1M KOH	[22]
Single layer CoAl LDH nanosheets	0.767	1.597	1M KOH	[23]
NiFeV LDH nanosheets	0.595	1.425	1M KOH	[24]
CoNiP/NiFe LDH	0.61	1.44	1M KOH	[25]
NiFe ₂ O ₄ NF	0.903	1.67	0.1M KOH	[26]
IrO ₂	0.74	1.52	0.1M KOH	[27]
NiFe LDHs	0.7	1.53	1M KOH	[28]
MoFe/NiOOH	0.703	1.51	1M KOH	[29]
RGO/MoS ₂ /Pd	0.645	1.475	1M KOH	[30]

The following equations were used for the conversion to the SHE scale (Tables 5-8): E (vs SHE) = 0.4 + η , where η is the value of the overpotential that is reported in literature; E (vs SHE) = E(vs RHE) - 0.059*pH (pH of 1M KOH is 14; pH of 0.1M KOH is 13).

Table S6. UOR performance of selected electrocatalysts.

Anode	E_{onset} (reported)	E (V vs SHE)	E (V vs RHE)	Electrolyte	Ref.
Direct electrooxidation					
CeO ₂ modified NiMoO ₄ nanosheets	0.31V vs Ag/AgCl	0.515	1.341	1M KOH + 0.33M Urea	[31]
MnCo ₂ O _{4.5} @Ni(OH) ₂ nanosheet	0.19V vs Ag/AgCl	0.395	1.221	5M KOH + 0.33M Urea	[32]
NiClOH-derived catalyst (NiClO-D)	1.34V vs RHE	0.514	1.34	1M KOH + 0.33M Urea	[33]
NiSn nanoparticle-incorporated carbon nanofibers	0.35V vs Ag/AgCl (12°C) 0.175V vs Ag/AgCl (55 °C)	0.555 0.38	1.381 1.206	1M KOH + 1M Urea	[34]
NiMo nanotube array	1.36V vs RHE	0.516	1.36	1M KOH + 0.1M Urea	[35]
Ni-Fe hollow cages	1.37V vs RHE	0.54	1.37	1M KOH + 0.5M Urea	[36]
Co-Fe hollow cages	1.4V vs RHE	0.57	1.4	1M KOH + 0.5M Urea	[36]
Ni _{1.5} Mn _{1.5} O ₄	0.29V vs Ag/AgCl	0.495	1.321	1M KOH + 0.33M Urea	[37]
NiCo LDH-NO ₃	0.37V vs Hg/HgO	0.535	1.361	1M KOH + 0.33M Urea	[38]
Ni-MOF nanowires	0.36V vs Ag/AgCl	0.565	1.391	1M KOH + 0.5M Urea	[39]
Highly porous pomegranatelike Ni/C	1.33V vs RHE	0.504	1.33	1M KOH + 0.33M Urea	[40]
Nickel nitride bead-like nanospheres array supported on Ni foam	1.34 vs RHE	0.514	1.34	1M KOH + 0.5M Urea	[41]
NiCo (20% Co) bimetallic nanoparticles	0.31V vs Hg/HgO	0.475	1.301	1M KOH + 0.33M Urea	[42]
Ni-Co (25% Co) bimetal decorated carbon nanotube aerogel	0.3V vs Ag/AgCl	0.505	1.331	1M KOH+ 1M Urea	[43]
Ni ₄₀ Cr ₄₀ /C	0.32V vs Ag/AgCl	0.525	1.351	1M KOH + 0.33M Urea	[44]
1% Fe; α -Ni(OH) ₂ /NF	1.312V vs RHE	0.486	1.312	1M KOH + 0.33M Urea	[45]
Ni(OH) ₂ with a monolayer of nanocup arrays	0.31V vs SCE	0.554	1.439	1M KOH + 0.33M Urea	[46]
Ni(OH) ₂ nanosheets	0.35V vs Hg/HgO	0.515	1.341	5M KOH + 0.33M Urea	[47]
Ni-foam supported Co(OH)F	1.25V vs RHE	0.424	1.25	1M KOH + 0.7M Urea	[48]

Table S7. AOR performance of selected electrocatalysts.

Anode	E (onset)	E (V vs SHE) onset peak	E (V vs RHE)	Electrolyte	Ref.
Transition metals-based catalysts					
Pt coated carbon fibres	-0.8V vs Hg/HgO	-0.635 -0.145	0.681	1M KOH + 0.1M NH ₃	[49]
Pt-decorated porous flower-like Ni NPs	~ 0.55V vs RHE	-0.276 -0.136	0.69	1M KOH + 0.1M NH ₃	[50]
Pt _x Eu alloys	-0.4V vs Ag/AgCl	-0.195 -0.045	0.781	1M KOH + 0.1M NH ₃	[51]
Zn-modified PtIr	0.3V vs RHE	-0.51 -0.20	0.62	0.5M KOH + 0.1M NH ₃	[52]
PtIr alloys	~ -0.6V vs Ag/AgCl	-0.395 -0.14	0.686	1M KOH + 1M NH ₃	[53]
PtRu alloys	~ -0.5V vs Ag/AgCl	-0.295 -0.1	0.726	1M KOH + 1M NH ₃	[53]
IrRh nanoparticles	-0.5V vs Hg/HgO	-0.335 -0.095	0.731	1M KOH + 2M NH ₃	[54]
Pt-NiO/C	~ -0.35 vs Ag/AgCl	-0.145 -0.025	0.801	1M KOH + 0.1M NH ₃	[55]
CeO ₂ -modified Pt	0.5V vs RHE	-0.326 -0.146	0.68	1M KOH + 0.1M NH ₃	[56]
Dendric Pt nanostructures	-0.45V vs SCE	-0.206 0.114	0.881	0.1M NaOH + 30mM NH ₃	[57]
Ni-based catalysts					
Ni(OH) ₂ /Ni foam	0.6V vs Hg/HgO	0.765	1.414	0.1M Na ₂ SO ₄ + 3mM NH ₃	[58]
Ni-Cu hydroxide nanowires	0.43V vs Ag/AgCl	0.635	1.461	0.5M NaOH + 55mM NH ₄ Cl	[59]
NiCu/C	0.4 vs Hg/HgO	0.565	1.391	1M KOH + 0.5M NH ₃	[60]
NiCr/C	0.4 vs Ag/AgCl	0.605	1.431	0.5M NaOH + 55mM NH ₄ Cl	[59]
NiMn/C	0.4 vs Ag/AgCl	0.605	1.431	0.5M NaOH + 55mM NH ₄ Cl	[59]
NiFe/C	0.4 vs Ag/AgCl	0.605	1.431	0.5M NaOH + 55mM NH ₄ Cl	[59]
NiCo/C	0.35 vs Ag/AgCl	0.555	1.381	0.5M NaOH + 55mM NH ₄ Cl	[59]
NiZn/C	0.45 vs Ag/AgCl	0.655	1.481	0.5M NaOH + 55mM NH ₄ Cl	[59]

Table S8. CO₂RR to CO performance of selected electrocatalysts in protic media.

Cathode	E j (mA cm ⁻²) FE (%)	E (V vs SHE)	E (V vs RHE)	Electrolyte	Ref.
Fe-Porphyrin-Based MOFs	-0.6V vs RHE -1.2 mA cm ⁻² 91%	-1.03	-0.6	0.5M KHCO ₃	[61]
Oxide-derived nanoporous Au	-0.3V vs RHE 90%	-0.7	-0.3	0.1M KHCO ₃	[62]
Electrodeposited Zn dendrites	-1.1V vs RHE -16 mA cm ⁻² 79%	-1.53	-1.1	0.5M NaHCO ₃	[63]
Ag/TiO ₂	-1.8V vs Ag/AgCl 90%	-1.6	-0.974	1M KOH	[64]
Ag/GDL	-0.96V vs RHE -343 mA cm ⁻² 100%	-1.79	-0.96	3M KOH	[65]
Ag/PTFE	-1V vs RHE -170 mA cm ⁻² >90%	-1.46	-1	1M KHCO ₃	[66]
Ag/carbon nanotubes	-0.75V vs RHE -350 mA cm ⁻² >95%	-1.58	-0.75	1M KOH	[67]
Au/C	-1.3V vs Ag/AgCl -10 mA cm ⁻² 90%	-1.1	-0.7	0.1M KHCO ₃	[68]
Dense Cu Nanowires	-0.3V vs RHE 60%	-0.7	-0.3	0.1M KHCO ₃	[69]
Ultrathin Au Nanowires	-0.35V vs RHE 94%	-0.78	-0.35	0.5M KHCO ₃	[70]
Oxide-derived Au NPs	-0.25V vs RHE -0.5 mA cm ⁻² 65%	-0.68	-0.25	0.5M NaHCO ₃	[71]
N-doped graphene quantum-dots-wrapped single-crystalline NPs	-0.25V vs RHE -2.5 mA cm ⁻² 93%	-0.68	-0.25	0.5M KHCO ₃	[72]

Table S9. CO₂RR to CO performance of selected electrocatalysts in aprotic media.

Cathode	E j (mA cm⁻²) FE (%)	E (V vs SHE)	Electrolyte	Ref.
Sn + BMIM-BF ₄ mediator	-1.45V vs NHE -120 mA cm ⁻² 97%	-1.45	ACN + 0.1M TBAPF ₆	[73]
In ^a	-2.6V vs Ag/AgCl 85%	-2.1	PC + 0.1M TEAP	[73]
Au + traces of water	-2.28V vs Fc/Fc ⁺ -4.5 mA cm ⁻² 80%	-1.9	ACN + 0.1M TEAP	[75]
Pd ^b	-2.5V vs Ag/AgCl 70%	-2.4	ACN + 0.1M TBAP	[76]
Cu ^a				
Ag ^a				
Au ^a	-2.8V vs Ag/AgCl selective formation	~ -2.3	PC + 0.1M TEAP	[74]
Zn ^a				
Sn ^a				
Sn ^a	-2.4V vs Ag/AgCl 100%	~ -1.8	PC + 0.1M TEAP	[77]
In ^a	-2.0V vs Ag/AgCl >95%	~ -1.4	PC + 0.1M TEAP	[77]
Pt + traces of water	-2.1V vs SHE 55% -1.9V vs SHE 68%	-2.1 -1.9	ACN + 0.1M TEAP	[78]

^aAg/AgCl (0.01m LiCl+0.1M TEAP)/PC was used as a reference electrode; ^bAg/Ag⁺ QRE was used as a reference electrode. The following equations were used for the conversion to SHE (Table 9 and 10): E^o(Fc/Fc⁺) ≈ 0.4V vs SHE [79]; E^o [Ag/AgCl(org)] ≈ 0.544 vs SHE [80, 81]; E^o (QRE) ≈ 0.1 vs SHE [1].

Table S10. Performance of selected electrocatalysts towards electrocarboxylation.

Cathode	Anode	Substrate	E Yield (%)	E (V vs SHE)	Electrolyte	Ref.
Ag foil	Pt	4- <i>i</i> -Bu-C ₆ H ₄ -CH(Cl)CH ₃	-2.6 vs SCE 61%	-2.36	DMF + 0.1M TBABF ₄	[82]
Ag foil	Pt	4- <i>i</i> -Bu-C ₆ H ₄ -CH(Cl)CH ₃	-2.4 vs SCE 75%	-2.16	DMF + 0.1 M TBABF ₄ + PP13 TFSI (50/50)	[82]
Ag foil	Pt	4- <i>i</i> -Bu-C ₆ H ₄ -CH(Cl)CH ₃	-1.75 vs SCE 82%	-1.51	PP13 TFSI	[82]
Ag	Pt	2-(1-chloroethyl)-6-methoxynaphthalene	-1.8 vs SCE 88.5%	-1.56	BMIM BF ₄	[83]
Ag	Al	PhCH ₂ Cl	-1.65 vs SCE 94%	-1.41	ACN + 0.1M TEAClO ₄	[84]
Hg	Al	PhCH ₂ Cl	-2.24 vs SCE 90%	-2.0	ACN + 0.1M TEAClO ₄	[84]
C	Al	PhCH ₂ Cl	-2.3 vs SCE 81%	-2.06	ACN + 0.1M TEAClO ₄	[84]
Ag	Al	4-CF ₃ -C ₆ H ₄ -CH ₂ Cl	-1.55 vs SCE 95%	-1.30	ACN + 0.1M TEAClO ₄	[84]
Ag	Al	PhCH ₃ CHCl	-1.68 vs SCE 80%	-1.44	ACN + 0.1M TEAClO ₄	[84]
Ag ₄₆ Cu ₄ ₀ Ni ₁₄	Mg	PhCH ₂ Br	-2.1 vs Ag/AgCl 95%	-1.9	DMF + 0.1M TBABF ₄	[85]
GC	Mg	PhCH ₃ CHCl	-1.59 vs SCE 66%	-1.35	DMF + 0.1M TEAI	[86]
CuNi alloy	Al	PhCH ₂ Br	-1.4 vs Ag 39.5%	-1.31	BMIMBF ₄	[87]
C	Al	NCCH ₂ Cl	-2.05 vs SCE 75%	-1.81	DMF + 0.1M TBAP	[88]
Hg	Al	NCCH ₂ Cl	-1.67 vs SCE 93%	-1.43	ACN + 0.1M TBAP	[88]
Pt	Mg	PhCH ₂ Cl	-2.2 vs Fc/Fc ⁺ 40%	-1.8	[DEME][TFSI]	[89]
Ag/C	Pt	PhCH ₃ CHBr	-1.4 vs Ag _w 94%	-1.31	ACN + 0.1 TBAB	[1]

Experimental electroanalytical evaluation of AOR- and UOR- based electrolyzers

Table S11. Electrochemical performance data for the electro-reduction of CO₂ to CO at Ag coated GDL cathode coupled to the oxygen evolution reaction and urea oxidation reaction at Ni foam anode in the flow cell.

j (mA cm ⁻²)	OER (V vs SHE)	UOR (V vs SHE)	CO ₂ RR (V vs SHE)	E _{cell} (V) [CO ₂ RR OER]	E _{cell} (V) [CO ₂ RR UOR]	ΔE (mV)
1	0.73	0.53	-	-	-	-
5	0.77	0.58	-1.3	2,07	1,88	190
10	0.80	0.60	-1.39	2,19	1,99	200
20	0.83	0.64	-1.45	2,28	2,09	190
40	0.88	0.70	-1.52	2,40	2,22	180
50	0.92	0.74	-1.58	2,5	2,32	180
100	1.0	0.82	-1.71	2,71	2,53	180

S _{geometrical} (Ag/GDL) = 1 cm², **S** _{geometrical} (Ni foam) = 1 cm², catholyte = 5M KOH; and anolyte = 5M KOH, 5M KOH + 0.33M Urea.

Table S12. Electrochemical performance data for the electro-reduction of CO₂ to CO and electrocarboxylation of (1-bromoethyl)benzene at Ag coated carbon paper cathode coupled to the oxygen evolution reaction and urea oxidation reaction at Ni foam anode in the H-cell.

j (mA cm ⁻²)	OER (V vs SHE)	UOR (V vs SHE)	CO ₂ RR (V vs SHE)	ECR (V vs SHE)	E _{cell} (V) [CO ₂ RR OER]	E _{cell} (V) [CO ₂ RR UOR]	E _{cell} (V) [ECR OER]	E _{cell} (V) [ECR UOR]
5	0.68	0.46	-1.18	-0.37	1.86	1.64	1.05	0.83
10	0.69	0.48	-1.31	-0.52	2	1.79	1.21	1
15	0.70	0.50	-1.39	-0.69	2.09	1.89	1.39	1.19
20	0.71	0.51	-1.5	-0.76	2.21	2.01	1.47	1.27
30	0.73	0.53	-1.63	-0.86	2.36	2.16	1.59	1.39
40	0.74	0.54	-1.74	-1.01	2.48	2.28	1.75	1.55
60	0.76	0.55	-1.97	-1.3	2.73	2.52	2.06	1.85
80	0.77	0.57	-2.18	-1.59	2.95	2.75	2.36	2.16

S _{geometrical} (Ag/C) = 0.15 cm², **S** _{geometrical} (Ni foam) = 0.15 cm², catholyte = 0.1M TBABr, 0.1M TBABr + 0.05M (1-bromoethyl)-benzene; and anolyte = 5M KOH, 5M KOH + 0.33M Urea.

Table S13. Energy savings for the electroreduction of CO₂ to CO and electrocarboxylation of (1-bromoethyl)benzene at Ag coated carbon paper cathode, coupled to the oxygen evolution reaction and urea oxidation reaction at Ni foam anode in the H-cell.

j (mA cm ⁻²)	Reference point: [CO ₂ RR OER]	ΔE (mV) [CO ₂ RR UOR]	ΔE (mV) [EC OER]	ΔE (mV) [EC UOR]
5	0	220	810	1030
10	0	210	790	1000
15	0	200	700	900
20	0	200	740	940
30	0	200	770	970
40	0	200	730	930
60	0	210	670	880
80	0	200	590	790

Table S14. Performance of Pt/C anode towards OER and AOR, and Ag/C cathode towards CO₂RR: electrode potentials as a function of total current density. Comparison of fresh Pt/C catalyst activity towards AOR with the activity after 1h, 2h and 3h of operation, respectively.

j (mA cm ⁻²)	OER (V vs SHE)	AOR (1 st cycle) (V vs SHE)	AOR (2 nd cycle) (V vs SHE)	AOR (3 rd cycle) (V vs SHE)	AOR (4 th cycle) (V vs SHE)	CO ² RR (V vs SHE)
0.1	-	-0.13	0.23	0.36	0.45	-
0.5	-	0	0.59	0.62	0.7	-0.55
1	0.71	0.2	0.77	0.73	0.78	-0.95
2	0.82	0.55	0.87	0.80	0.86	-1.05
5	1.08	0.89	0.99	0.91	1.03	-1.18
10	1.38	1.05	1.25	1.27	1.45	-1.31

S_{geometrical} (Ag/C cathode) = 1 cm², **S**_{geometrical} (Pt/C anode) = 1 cm², catholyte = 0.1M TBABr; and anolyte = 5M KOH, 5M KOH + 1M Ammonia.

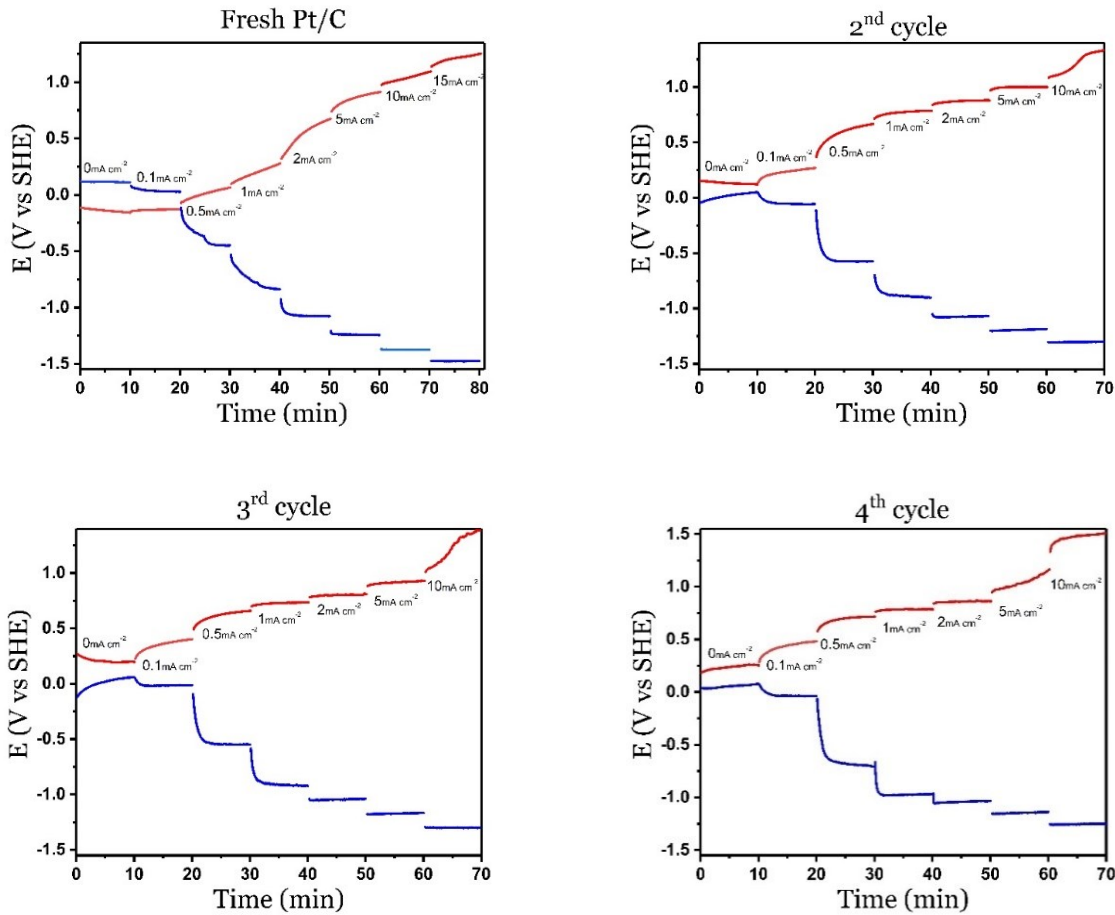


Figure S1. Evaluation of the catalyst stability. Chronopotentiometry curves recorded for the oxidation of 1M Ammonia in 5M KOH at Pt/C anode (red trace), and for the reduction of CO₂ in ACN + 0.1M TBABr at Ag cathode (blue trace) in H-cell at different current densities (0-15 mA cm⁻²).

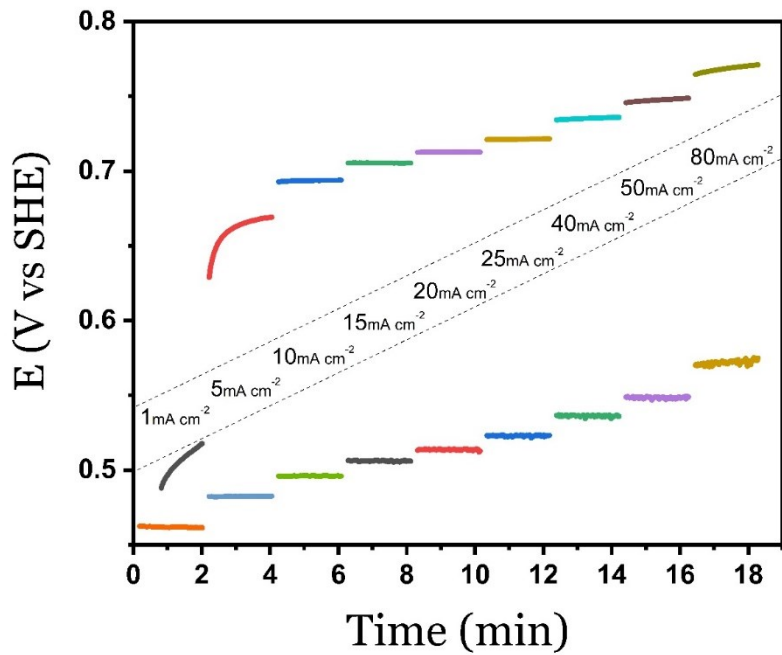


Figure S2. Chronopotentiometry curves for the oxidation of 0.33M Urea and OER at Ni anode in H-cell in 5M KOH at different current densities (1-80 mA cm^{-2}).

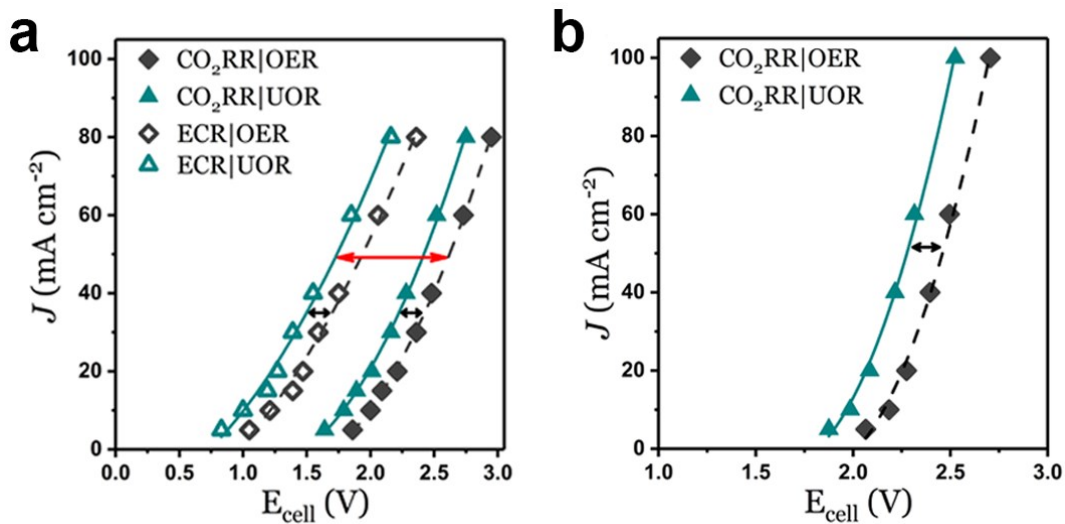


Figure S3. Performance of [CO₂RR|UOR] (a,b) and [ECR|UOR] (a) electrolyzers compared with OER-based analogues. Total current density as a function of the cell potential for batch (a) and flow (b) electrolyzers.

Table S15. Summarized results of direct CO₂RR and ECR at arbitrary potentials/current densities.

Entry	System	J , (mA cm ⁻²)	E(cathode), V vs. SHE	E_{cell} , V	FE/Yield, %
1 ^a	[ECR UOR]	40 ^c	-1.3	1.8V	86±4 ^d (90)
2 ^b	[CO ₂ RR _{org} UOR]	40	-1.7	2.3V	90±3 ^d (93)
3 ^b	[CO ₂ RR _{aq} UOR]	100	-1.7	2.5V	87±3 ^d (90)

^aElectrolysis was performed at constant potential. ^bElectrolysis was performed at constant current density. ^cValue corresponds to the current density observed in first 30 minutes of electrolysis; further decrease in current density is associated with reagent (R-Br) depletion. ^dReactions were repeated several times, average combined yields of ECR products and FE of CO with standard deviations are reported (maximum values are shown in brackets)

References:

1. J. J. Medvedev, X. V. Medvedeva, F. Li, T. A. Zienchuk and A. Klinkova, *ACS Sustainable Chem. Eng.*, 2019, **7**, 19631-19639.
2. J. A. Dean, *Langes Handbook of Chemistry Fifteenth Edition*, McGraw-Hill Inc, New York, 1999.
3. K. G. Joback and R. C. Reid, *Chem. Eng. Commun.*, **57**, 233-243, (1987).
4. Chemeo: chemical and physical properties prediction, <https://www.chemeo.com/predict?smiles=CCCC>.
5. G. Milazzo and M. Blank, *M. Bioelectrochemistry I: Biological Redox Reactions*, Plenum Press, New York, 1983.
6. Lide, D. in *CRC Handbook of Chemistry and Physics*, CRC Press, Boca Raton Fl., 2007.
7. J. K. Nørskov, F. Studt, F. Abild-Pedersen and T. Bligaard, *Fundamental Concepts in Heterogeneous Catalysis*, John Wiley & Sons, Inc., Hoboken, 2014.
8. S. Nitopi, E. Bertheussen, S.B. Scott, X. Liu, A.K. Engstfeld, S. Horch, B. Seger, I.E. Stephens, K. Chan, C. Hahn and J.K. Nørskov, *Chem. Rev.* 2019, **119**, 7610-7672.
9. H. Oberhofer, in In: *Handbook of Materials Modeling*. ed. W. Andreoni and S. Yip, Springer, Cham, 2018.
10. A. A. Peterson, F. Abild-Pedersen, F. Studt, J. Rossmeisl, J. K. Nørskov. *Energy Environ. Sci.*, 2010, **3**, 1311-1315.
11. S. Nitopi, E. Bertheussen, S. B. Scott, X. Liu, A. K. Engstfeld, S. Horch, B. Seger, I. E. L. Stephens, K. Chan, C. Hahn, J. K. Nørskov, T. F. Jaramillo, I. Chorkendorff, *Chem. Rev.*, 2019, **119**, 7610-7672.
12. Z. Sun, T. Ma, H. Tao, Q. Fan, B. Han, *Chem*, 2017, **3**, 560-587.
13. Y. Matsubara, *ACS Energy Lett.*, 2017, **2**, 1886-1891.
14. N.-T. Suen, S.-F. Hung, Q. Quan, N. Zhang, Y.-J. Xu, H. M. Chen, *Chem. Soc. Rev.*, 2017, **46**, 337-365.
15. N. M. Adli, H. Zhang, S. Mukherjee, G. Wu, *J. Electrochem. Soc.*, 2018, **165**, J3130-J3147.

16. Y.-F. Huang, D.-Y. Wu, A. Wang, B. Ren, S. Rondinini, Z.-Q. Tian, C. Amatore, *J. Am. Chem. Soc.*, 2010, **132**, 17199-17210.
17. Z. Liu, N. Li, H. Zhao, Y. Zhang, Y. Huang, Z. Yin, Y. Du, *Chem. Sci.*, 2017, **8**, 3211-3217.
18. Z. Cai, D. Zhou, M. Wang, S. Bak, Y. Wu, Z. Wu, Y. Tian, X. Xiong, Y. Li, W. Liu, *Angew. Chem.*, 2018, **130**, 9536-9540.
19. B. Zhang, X. Zheng, O. Voznyy, R. Comin, M. Bajdich, M. Garcia-Melchor, L. Han, J. Xu, M. Liu, L. Zheng, F. P. G. de Arquer, C. T. Dinh, F. Fan, M. Yuan, E. Yassitepe, N. Chen, T. Regier, P. Liu, W. Li, P. D. Luna, A. Vojvodic, E. H. Sargent, *Science*, 2016, **352**, 333-337.
20. Z. Li, M. Shao, H. An, Z. Wang, S. Xu, M. Wei, D. G. Evans, X. Duan, *Chem. Sci.*, 2015, **6**, 6624-6631.
21. X. Li, J. Zhou, X. Li, M. Xin, T. Cai, W. Xing, Y. Chai, Q. Xue, Z. Yan, *Electrochim. Acta*, 2017, **252**, 275-285.
22. F. Song, X. Hu, *J. Am. Chem. Soc.*, 2014, **136**, 16481-16484.
23. H. Li, T.-N. Tran, B.-J. Lee, C. Zhang, J.-D. Park, T.-H. Kang, J.-S. Yu, *ACS Appl. Mater. Interfaces*, 2017, **9**, 20294-20298.
24. P. Li, X. Duan, Y. Kuang, Y. Li, G. Zhang, W. Liu, X. Sun, *Adv. Energy Mater.*, 2018, **8**, 1703341.
25. L. Zhou, S. Jiang, Y. Liu, M. Shao, M. Wei, X. Duan, *ACS Appl. Energy Mater.*, 2018, **1**, 623-631.
26. M. Li, Y. Xiong, X. Liu, X. Bo, Y. Zhang, C. Han, L. Guo, *Nanoscale*, 2015, **7**, 8920-8930.
27. S. Anantharaj, P. E. Karthik, S. Kundu, *J. Mater. Chem. A.*, 2015, **3**, 24463-24478.
28. F. Song, X. Hu, *Nature Commun.*, 2014, **5**, 4477.
29. Y. Jin, S. Huang, X. Yue, H. Du, P. K. Shen, *ACS Catal.*, 2018, **8**, 2359-2363.
30. A. Pandey, A. Mukherjee, S. Chakrabarty, D. Chanda, S. Basu, *ACS Appl. Mater. Interfaces*, 2019, **11**, 42094-42103.
31. W. Gao, C. Wang, F. Ma, D. Wen, *Electrochim. Acta*, 2019, **320**, 134608.
32. L. Sha, K. Ye, J. Yin, K. Zhu, K. Cheng, J. Yan, G. Wang, D. Cao, *Chem. Eng. J.*, 2020, **381**, 122603.
33. L. Zhang, L. Wang, H. Lin, Y. Liu, J. Ye, Y. Wen, A. Chen, L. Wang, F. Ni, Z. Zhou, S. Sun, Y. Li, B. Zhang, H. Peng, *Angew. Chem. Int. Ed.*, 2019, **58**, 16820-16825.
34. N. A. M. Barakat, M. T. Amen, F. S. Al-Mubaddel, M. R. Karim, M. Alrashed, *J. Adv. Res.*, 2019, **16**, 43-53.
35. J.-Y. Zhang, T. He, M. Wang, R. Qi, Y. Yan, Z. Dong, H. Liu, H. Wang, B. Y. Xia, *Nano Energy*, 2019, **60**, 894-902.
36. Y. Feng, X. Wang, P. Dong, J. Li, L. Feng, J. Huang, L. Cao, L. Feng, K. Kajiyoshi, C. Wang, *Sci. Reports*, 2019, **9**, 15965.
37. S. Periyasamy, P. Subramanian, E. Levi, D. Aurbach, A. Gedanken, A. Schechter, *ACS Appl. Mater. Interfaces*, 2016, **8**, 12176-12185.
38. M. Zeng, J. Wu, Z. Li, H. Wu, J. Wang, H. Wang, L. He, X. Yang, *ACS Sustainable Chem. Eng.*, 2019, **7**, 4777-4783.
39. M. Yuan, R. Wang, Z. Sun, L. Lin, H. Yang, H. Li, C. Nan, G. Sun, S. Ma, *Inorg. Chem.*, 2019, **58**, 11449-11457.
40. L. Wang, L. Ren, X. Wang, X. Feng, J. Zhou, B. Wang, *ACS Appl. Mater. Interfaces*, 2018, **10**, 4750-4756.

41. S. Hu, C. Feng, S. Wang, J. Liu, H. Wu, L. Zhang, J. Zhang, *ACS Appl. Mater. Interfaces*, 2019, **11**, 13168-13175.
42. W. Xu, H. Zhang, G. Li, Z. Wu, *Sci. Reports*, 2014, **4**, 5863.
43. R. M. Tesfaye, G. Das, B. J. Park, J. Kim, H. H. Yoon, *Sci. Reports*, 2019, **9**, 479.
44. R. K. Singh, A. Schechter, *ChemCatChem*, 2017, **9**, 3374-3379.
45. J. Xie, W. Liu, F. Lei, X. Zhang, H. Qu, L. Gao, P. Hao, B. Tang, Y. Xie, *Chem. Eur. J.*, 2018, **24**, 18408-18412.
46. M.-S. Wu, R.-Y. Ji, Y.-R. Zheng, *Electrochim. Acta*, 2014, **144**, 194-199.
47. D. Wang, W. Yan, G. G. Botte, *Electrochem. Commun.*, 2011, **13**, 1135-1138.
48. M. Song, Z. Zhang, Q. Li, W. Jin, Z. Wu, G. Fu, X. Liu, *J. Mater. Chem. A.*, 2019, **7**, 3697-3703.
49. A. M. Pourrahimi, R. L. Andersson, K. Tjus, V. Stöm, A. Björk, R. T. Olsson, *Sustainable Energy Fuels*, 2019, **3**, 2111-2124.
50. J. Liu, B. Chen, Y. Kou, Z. Liu, X. Chen, Y. Li, Y. Deng, X. Han, W. Hu, C. Zhong, *J. Mater. Chem. A.*, 2016, **4**, 11060-11068.
51. Y. Kang, W. Wang, J. Li, C. Hua, S. Xue, Z. Lei, *Int. J. Hydrogen Energy*, 2017, **42**, 18959-18967.
52. J. Jiang, *Electrochem. Commun.*, 2017, **75**, 52-55.
53. K. Endo, K. Nakamura, Y. Katayama, T. Miura, *Electrochim. Acta*, 2004, **49**, 2503-2509.
54. J. C. M. Silva, M. H. M. Assumpcao, P. Hammer, A. O. Neto, E. V. Spinace, E. A. Baranova, *ChemElectroChem*, 2017, **4**, 1101-1107.
55. Y. Kang, W. Wang, J. Li, Q. Li, S. Liu, Z. Lei, *J. Electrochem. Soc.*, 2017, **164**, F958-F965.
56. K. Siddharth, Y. Chan, L. Wang, M. Shao, *Curr. Opinion Electrochem.*, 2018, **9**, 151-157.
57. J.-Y. Ye, J.-L. Lin, Z.-Y. Zhou, Y.-H. Hong, T. Sheng, M. Rauf, S.-G. Sun, *J. Electroanal. Chem.*, 2018, **819**, 495-501.
58. Y.-J. Shin, Y.-H. Huang, C. P. Huang, *Electrochim. Acta*, 2018, **263**, 261-271.
59. W. Xu, R. Lan, D. Du, J. Humphreys, M. Walker, Z. Wu, H. Wang, S. Tao, *Appl. Cat. B: Environmental*, 2017, **218**, 470-479.
60. H. Zhang, Y. Wang, Z. Wu, and D. Y. C. Leung, *Energy Procedia*, 2017, **142**, 1539-1544.
61. B.-X. Dong, S.-L. Qian, F.-Y. Bu, Y.-C. Wu, L.-G. Feng, Y.-L. Teng, W.-L. Liu, Z.-W. Li, *ACS Appl. Energy Mater.*, 2018, **1**, 4662-4669.
62. Z. Qi, J. Biener, M. Biener, *ACS Appl. Energy Mater.*, 2019, **2**, 7717-7721.
63. J. Rosen, G. S. Hutchings, Q. Lu, R. V. Forest, A. Moore, F. Jiao, *ACS Catal.*, 2015, **5**, 4586-4591.
64. S. Ma, Y. Lan, G. M. J. Perez, S. Moniri, P. J. A. Kenis, *ChemSusChem*, 2014, **7**, 866-874.
65. S. Verma, X. Lu, S. Ma, R. I. Masel, P. J. A. Kenis, *Phys. Chem. Chem. Phys.*, 2016, **18**, 7075-7084.
66. C.-T. Dihn, F. P. D. de Arquer, D. Sinton, E. H. Sargent, *ACS Energy Lett.*, 2018, **3**, 2835-2840.
67. S. Ma, R. Luo, J. I. Gold, A. Z. Yu, B. Kim, P. J. A. Kenis, *J. Mater. Chem. A.*, 2016, **4**, 8573-8578.
68. H. T. Ahangari, T. Portail, A. T. Marshall, *Electrochem. Commun.*, 2019, **101**, 78-81.

69. D. Raciti, K. J. Livi, C. Wang, *Nano Lett.*, 2015, **15**, 6829-6835.
70. W. Zhu, Y.-J. Zhang, H. Zhang, H. Lv, Q. Li, R. Michalsky, A. A. Peterson, S. Sun, *J. Am. Chem. Soc.*, 2014, **136**, 16132-16135.
71. Y. Chen, C. W. Li, M. W. Kanan, *J. Am. Chem. Soc.*, 2012, **134**, 19969-19972.
72. J. Fu, Y. Wang, J. Liu, K. Huang, Y. Chen, Y. Li, J.-J. Zhu, *ACS Energy Lett.*, 2018, **3**, 946-951.
73. I. Ganesh, *J. Phys. Chem. C.*, 2019, **123**, 30198-30212.
74. S. Ikeda, T. Takagi, K. Ito, *Bull. Chem. Soc. Jpn.*, 1987, **60**, 2517-2522.
75. Y. Tomita, S. Teruya, O. Koga, Y. Hori, *J. Electrochem. Soc.*, 2000, **147**, 4164-4167.
76. K. Ohkawa, Y. Noguchi, S. Nakayama, K. Hashimoto, A. Fujishima, *J. Electroanal. Chem.*, 1994, **369**, 247-250.
77. K. Ito, S. Ikeda, N. Yamanuchi, T. Iida, T. Takagi, *Bull. Chem. Soc. Jpn.*, 1985, **58**, 3027-3028.
78. Y. Tomita, Y. Hori, *Studies Surf. Sci. Catal.*, 1998, **114**, 581-584.
79. R. R. Gagne, C. A. Koval, G. C. Lisensky, *Inorg. Chem.*, 1980, **19**, 2854-2855.
80. O. Hammerich, V. D. Parker, *Electrochim. Acta.*, 1973, **18**, 537-541.
81. M. Oyama, *Rev. Polarography*, 2004, **50**, 19-42.
82. S. Mena, J. Sanchez, G. Guirado, *RSC. Adv.*, 2019, **9**, 15115-15123.
83. S. Mena, S. Santiago, I. Gallardo, G. Guirado, *Chemosphere*, 2020, **245**, 125557.
84. A. A. Isse, A. Gennaro, *Chem. Commun.*, 2002, 2798-2799.
85. V. Rajagopal, P. Manivel, N. Nesakumar, M. Kathiresan, D. Velayutham, V. Suryanarayanan, *ACS Omega*, 2018, **3**, 17125-17134.
86. B.-L. Chen, H.-W. Zhu, Y. Xiao, Q.-L. Sun, H. Wang, J.-X. Lu, *Electrochem. Commun.*, 2014, **42**, 55-59.
87. D. Yimin, N. Lanli, L. Hui, Z. Jiaqi, Y. Linping, F. Qiuju, *Int. J. Electrochem. Sci.*, 2018, **13**, 1084-1095.
88. A. A. Isse, A. Gennaro, *J. Electrochem. Soc.*, 2002, **149**, D113-D117.
89. H. Tateno, K. Nakabayashi, T. Kashiwagi, H. Senboku, M. Atobe, *Electrochim. Acta.*, 2015, **161**, 212-218.